



Photoelectrochemical Properties of CdS/CdSe Sensitized TiO₂ Nanocable Arrays



Peng Wang^a, Yu Zhang^{a,b,*}, Liang Su^a, Wenzhu Gao^b, Baolin Zhang^a, Hairong Chu^c,
Yiding Wang^a, Jun Zhao^{d,e}, William W. Yu^{a,d,e,*}

^a State Key Laboratory on Integrated Optoelectronics, College of Electronic Science and Engineering, Jilin University, Changchun 130012, China

^b State Key Laboratory of Superhard Materials, College of Physics, Jilin University, Changchun 130012, China

^c Changchun Institute of Optics, Fine Mechanics and Physics, Chinese Academy of Sciences, Changchun 130025, China

^d Department of Chemistry and Physics, Louisiana State University, Shreveport, LA 71115, USA

^e College of Material Science and Engineering, Qingdao University of Science and Technology, Qingdao 266042, China

ARTICLE INFO

Article history:

Received 27 December 2014

Received in revised form 24 February 2015

Accepted 28 February 2015

Available online 3 March 2015

Keyword:

Nanocable
Electrodeposition
Sensitization
Photocurrent

ABSTRACT

Vertically aligned TiO₂/CdS and TiO₂/CdS/CdSe nanocable arrays on fluorine-doped tin oxide (FTO) were fabricated by electrochemical deposition of CdS and CdS/CdSe shells over TiO₂ nanorod arrays. The morphology, composition, structure and optical absorbance of CdS and CdS/CdSe shells sensitized TiO₂ nanorod arrays were characterized by different analytical methods. The CdS shell with a hexagonal structure and the CdSe shell with a face-centered structure were densely and uniformly coated on the tetragonal TiO₂ nanorod cores both radially and longitudinally. The photovoltaic measurement showed that the photocurrent density obtained under AM1.5G illumination with a zero bias potential (Ag/AgCl electrode) largely increased from 2.17 to 6.57 mA/cm², when the TiO₂/CdS nanocables were further covered by the CdSe shell.

© 2015 Elsevier Ltd. All rights reserved.

1. Introduction

To meet the increasing demand of energy, it is important to research into new resources. Quantum dot-sensitized solar cells (QDSSCs) have been considered as one of the promising power sources due to their simple fabrication procedure, low cost and high conversion efficiency [1]. TiO₂ nanocrystal films have been widely applied in photovoltaic conversion techniques and photocatalysis applications [2]. Especially, one-dimensional single crystalline TiO₂ arrays provide direct electrical pathways to improve the transportation of photogenerated electrons; TiO₂ nanotubes [3], nanorods [4] and nanowires [5,6] have received more attention than polycrystalline ones. However, it has been widely known that TiO₂ has a large band gap of 3.2 eV limiting its absorption in the ultraviolet region which is only about 3–5% of all the solar spectrum energy.

Recently, inorganic semiconductor quantum dots (QDs) of narrow band gap, such as CdS, [4,7] CdSe, [8,9] CdTe, [10] PbS [11] and PbSe, [12,13] have attractively been used for QDSSCs. Among

them, CdS and CdSe are typical direct band gap semiconductors with the band gap of 2.25 and 1.70 eV respectively, which means that the sensitization with CdS or CdSe can broaden the light absorption range compared to pure TiO₂. Compared with CdS or CdSe sensitized TiO₂ separately, co-sensitization of TiO₂ films with both CdS and CdSe QDs can hugely tune the response of the photoanode in the visible light region, promote the charge separation and the transportation of photo-generated electrons, and finally improve the photoelectric performance [14,15]. Different kinds of methods have been proposed for the sensitization of TiO₂ nanostructures with QDs, such as direct growth by chemical bath deposition (CBD) [16,17], successive ionic layer adsorption and reaction (SILAR) [18,19], assembly of QDs by immobilization via organic linkers, [20] and electrochemical method [21]. Previously, Zhang and co-workers fabricated the ZnO/CdS/CdSe electrode by the CBD; [22] Luo and co-workers made CdTe QDs sensitized TiO₂ nanorod array film photoanodes via the route of electrochemical atomic layer deposition; [23] and Li et al. prepared ZnO/CdTe core-shell nanocable arrays on indium-tin-oxide (ITO) using electrochemical method [24]. However, few works have demonstrated the CdS/CdSe co-sensitized nanocrystalline TiO₂ nanorod arrays by electrodeposition.

We report here a facile and labor saving electrodeposition method to deposit CdS and CdS/CdSe shells over the TiO₂ nanorod

* Corresponding authors.

E-mail addresses: yuzhang@jlu.edu.cn (Y. Zhang), wuyu6000@gmail.com (W.W. Yu).

arrays to prepare the TiO_2/CdS and the $\text{TiO}_2/\text{CdS}/\text{CdSe}$ nanocable arrays on fluorine-doped tin oxide (FTO) coated glass substrates. The detailed synthesis process, characterization, and photoelectrochemical properties of these photoelectrodes were discussed, while the performances of TiO_2/CdS and $\text{TiO}_2/\text{CdS}/\text{CdSe}$ nanocable arrays were compared and analyzed. Before deposited with the CdSe shell, the CdS shell had already been coated perfectly over the TiO_2 surface without any blank areas, thus we got the structure which promoted the photo-excited electron transfer following the process as we designed: from CdSe to CdS, and then to TiO_2 . These electrodes performed an obvious photocurrent density of $6.57 \text{ mA}/\text{cm}^2$ under AM1.5G illumination with an output potential difference of 1.04 V.

2. Experimental

2.1. Preparation of TiO_2 nanorod arrays

The TiO_2 nanorod arrays were prepared by a hydrothermal synthesis method which was similar to a previous report [25]. Firstly, 60 mL of deionized water was mixed with 60 mL of concentrated hydrochloric acid (mass fraction 36.5–38%). With continuously stirring at room temperature, 2 mL of titanium butoxide was added. After it was stirred for 30 min, 30 mL of the mixture was placed in a Teflon-liner stainless steel autoclave of 100 mL volume. Then, three pieces of FTO substrates ($15 \Omega/\text{square}$), ultrasonically cleaned for 60 min in a mixed solution of deionized water, acetone, and 2-propanol with a volume ratio of 1:1:1, were placed in the Teflon-liner with an angle against the wall and the FTO sides faced down. The hydrothermal synthesis was conducted at 140°C for 14 h in an electric oven. After synthesis, the autoclave was cooled to room temperature in ambient air. The samples were

taken out, rinsed extensively with deionized water, and then dried at 150°C in an oven.

2.2. Preparation of TiO_2/CdS nanocable arrays

The electrodeposition of the CdS shell was then carried out using an electrochemical workstation (Corrtest CS150) with a three-electrode system. The TiO_2 nanorod array-on-FTO, a standard Ag/AgCl electrode, and Pt foil were used as the working electrode, the reference electrode, and the counter electrode, respectively. The electrolyte mixed with 0.2 M of $\text{Cd}(\text{NO}_3)_2$ and 0.2 M of thiourea in a 1/1 (v/v) dimethyl sulphoxide (DMSO)/water and was kept at 90°C in a water bath [21]. After 10–30 min of constant voltage electrodeposition at $0.66 \text{ V}/\text{cm}^2$, the TiO_2/CdS nanocable array was taken out and washed by deionized water and ethanol successively.

2.3. Preparation of $\text{TiO}_2/\text{CdS}/\text{CdSe}$ nanocable arrays

The electrolyte was mixed with 0.02 M of $\text{Cd}(\text{CH}_3\text{COOH})_2$, 0.04 M of ethylene diamine tetraacetic acid disodium salt (EDTA), and 0.02 M of Na_2SeSO_3 (prepared by refluxing 0.48 g of Se powder and 2.0 g of Na_2SO_3 in water at 100°C for 1 h) in deionized water, with the solution pH of 7.5–8. The electrodeposition was performed at $1 \text{ V}/\text{cm}^2$ for 15 min on the prepared TiO_2/CdS nanocable to get $\text{TiO}_2/\text{CdS}/\text{CdSe}$, followed by washing with water and drying in the open air.

2.4. Characterization

The microstructures of the samples were examined by using field emission scanning electron microscopy (FESEM, JEOL JSM-6700). The images of transmission electron microscope (TEM) and high resolution TEM (HRTEM) were taken by a JEM-2100F high-resolution transmission microscope operated at 200 kV. The absorption characterizations of the films were investigated by a UV-3600 double-beam spectrophotometer. A Rigaku D/max-2500 X-ray diffractometer with Cu $K\alpha$ radiation ($\lambda = 0.15418 \text{ nm}$) was used at room temperature to detect the crystal structure of the as-prepared samples. Photoelectrochemical measurements measured by an electrochemical workstation (Corrtest CS150) were performed in a polysulfide redox couple ($\text{S}^{2-}/\text{SO}_3^{2-}$) electrolyte containing 0.25 M Na_2S and 0.35 M Na_2SO_3 dissolved in deionized water, in which the TiO_2/CdS and $\text{TiO}_2/\text{CdS}/\text{CdSe}$ nanocable arrays on FTO, Pt foil, and Ag/AgCl electrode were

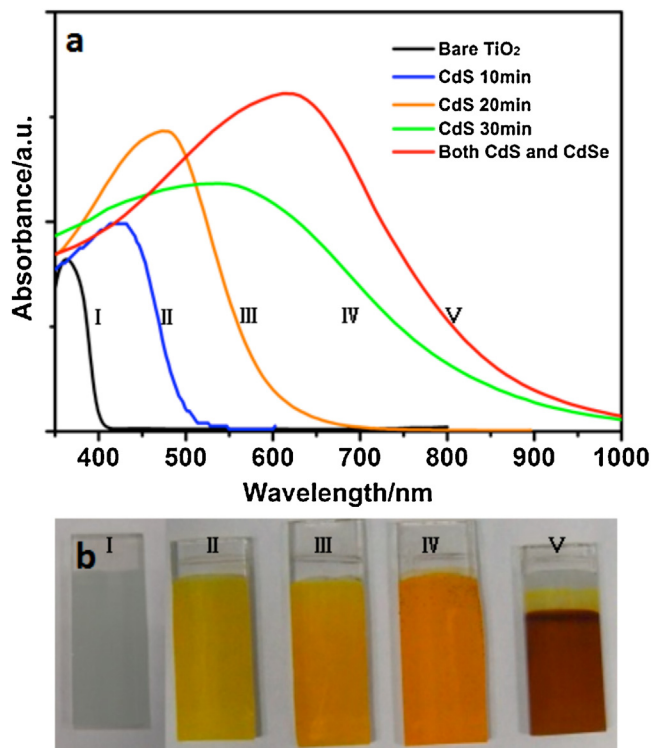


Fig. 1. UV-vis absorption spectra of bare TiO_2 nanorod arrays (black line), the TiO_2/CdS nanocable arrays with the depositing time of 10 (blue line), 20 (orange line) and 30 min (green line), and the $\text{TiO}_2/\text{CdS}/\text{CdSe}$ nanocable arrays with the depositing time of 20 min of each shell successively (a); The pictures of the samples (b). (For interpretation of the references to color in this figure legend, the reader is referred to the web version of this article.)

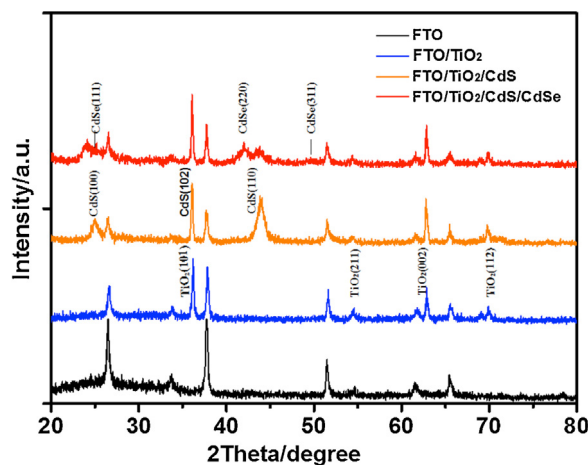


Fig. 2. XRD patterns of the FTO, TiO_2 nanorod arrays, TiO_2/CdS and $\text{TiO}_2/\text{CdS}/\text{CdSe}$ nanocable arrays. (For interpretation of the references to color in the text, the reader is referred to the web version of this article.)

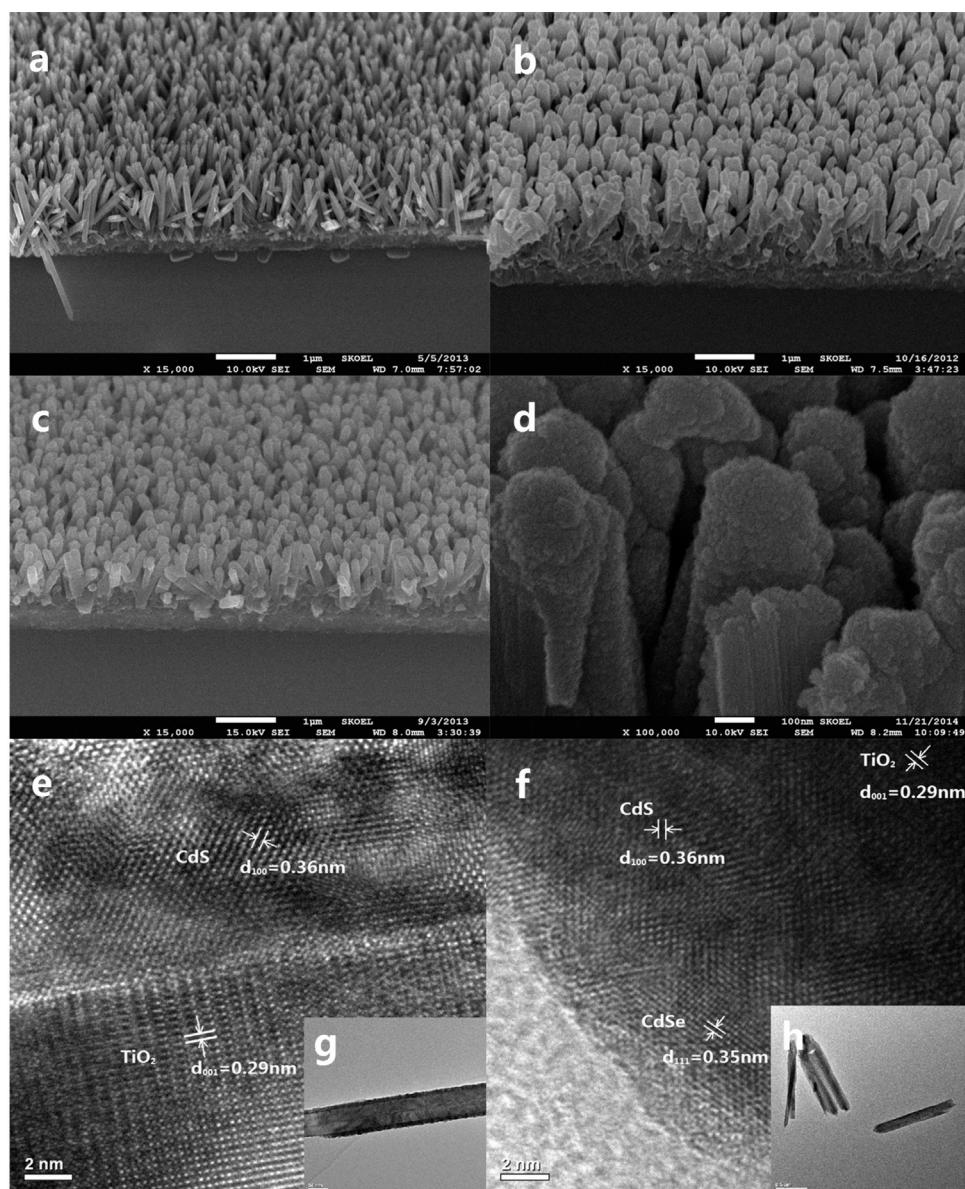


Fig. 3. SEM images of TiO_2 nanorod arrays (a), TiO_2/CdS nanocable arrays (b), and $\text{TiO}_2/\text{CdS}/\text{CdSe}$ nanocable arrays (c, d); typical HRTEM images of the TiO_2/CdS nanocables (e) and the $\text{TiO}_2/\text{CdS}/\text{CdSe}$ nanocables (f), showing the interface and crystalline structure of the nanocables; low-magnification TEM images showing the uniform morphology of the TiO_2/CdS nanocables (g) and the $\text{TiO}_2/\text{CdS}/\text{CdSe}$ nanocables (h).

used as the working electrode, the counter-electrode, and the reference electrode, respectively. An AM1.5G light with a power of $100 \text{ mW}/\text{cm}^2$ produced by a Zolix SS150 Solar Simulator was used as the illumination source.

3. Results and Discussion

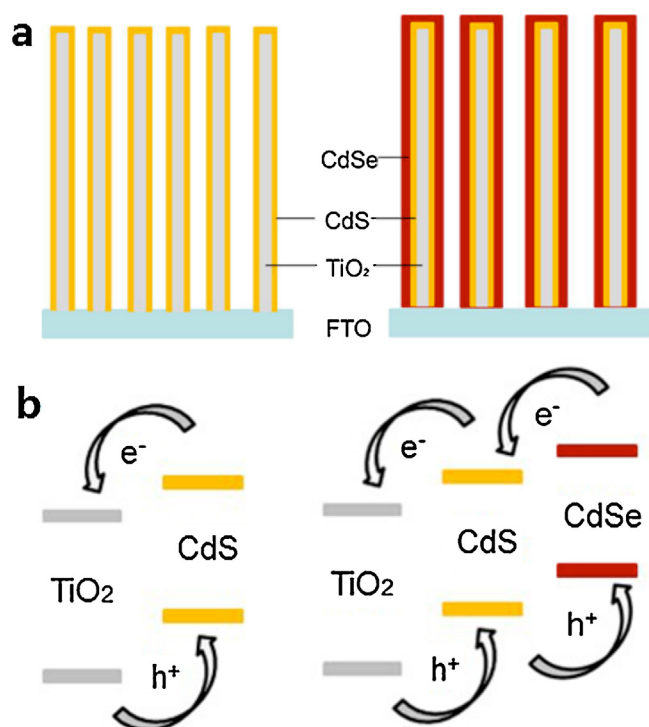
3.1. UV–vis absorption spectroscopy

The UV–vis absorption curves of the TiO_2 nanorod arrays, the TiO_2/CdS nanocable arrays with the CdS shells of different thicknesses and the $\text{TiO}_2/\text{CdS}/\text{CdSe}$ nanocable arrays are shown in Fig. 1a. The absorption of the TiO_2 nanorod arrays peaked at 380 nm (black line) had no obvious absorbance in the visible region for its large band gap (3.2 eV). There was a significantly red-shift of the peak. After the CdS shells were coated over the nanorod arrays, the absorption peak shifted to 440 (blue line), 480 (orange line) and 580 nm (green line) with longer CdS deposition time. As a

result, the absorption was broadened from 380 to 580 nm, indicating the effective photoabsorption for the ordered structure. Correspondingly, the color of TiO_2/CdS was yellow, and turned dark red with the increase of deposition time. The absorption peak shifted to red largely due to the large shell thickness, which demonstrated the band gap becomes small. With the growth of CdS/CdSe shells (dark-red color, Fig. 1b), a similar result was achieved which exhibited broader absorption bands from 350 to 650 nm. These variations indicated that the growth of CdS or CdS/CdSe shells significantly extended the spectra response of TiO_2 electrode to the visible light region. The improvement of absorbing visible light makes this type of core-shell nanocable arrays promising applications in photovoltaics.

3.2. Phase composition and phase structure

Fig. 2 shows the XRD patterns taken from the bare FTO substrate (black line), pure TiO_2 nanorod arrays (blue line), TiO_2/CdS



Scheme 1. (a) Schematic diagram of the TiO_2/CdS nanocable arrays and the $\text{TiO}_2/\text{CdS}/\text{CdSe}$ nanocable arrays, (b) electrode and charge-transfer processes in the two types nanocable array.

nanocable arrays (orange line) and $\text{TiO}_2/\text{CdS}/\text{CdSe}$ nanocable arrays (red line). For pure TiO_2 nanorod arrays, 4 different peaks were indexed to the (101), (211), (002) and (112) planes of tetragonal phase TiO_2 (JCPDS 88-1175). The predominant (101) and (002) peaks suggested that the TiO_2 nanorod arrays grew with their *c*-axis orientation normal to the FTO surface. After electrodeposition of CdS, two new peaks at 24.84° and 43.74° were indexed respectively to the (100) and (110) planes of the hexagonal CdS (JCPDS 77-2306), which were added to the diffraction peaks from the tetragonal TiO_2 nanorod arrays. Another peak around 36° could be indexed to both the (102) plane of the hexagonal CdS and the (101) plane of the tetragonal TiO_2 , was enhanced. With the electrodeposition of CdSe, there were three new peaks appeared at 25.38° , 42.04° and 67.14° which were assigned to the (111), (220) and (311) planes of cubic phase CdSe (JCPDS 19-191).

3.3. SEM images

The FESEM images of the TiO_2 nanorod arrays, the TiO_2/CdS nanocable arrays and the $\text{TiO}_2/\text{CdS}/\text{CdSe}$ nanocable arrays are shown in Fig. 3. Fig. 3a gives the tilted cross view of the pure TiO_2 nanorod arrays. In the image, the TiO_2 nanorod arrays, which covered uniformly and densely on the FTO substrate, are nearly vertical with the morphology of quadrangular prism that reveals the tetragonal crystal structure. Besides, the sides of the TiO_2 nanorod arrays are relatively smooth. Our nanorods had a length of $2\ \mu\text{m}$ and diameters between 80 and 120 nm, respectively, and a planar density of 8–12 wire/ μm^2 . The TiO_2/CdS nanocable arrays with the electrodeposition of CdS shells for 20 min are shown in the Fig. 3b. There was an obvious change between the pure TiO_2 nanorod arrays and the TiO_2/CdS nanocable arrays that their surfaces were no longer smooth. Meanwhile, after coated with the CdS shells, the appearance of the arrays were cylinders and the diameters became larger. Then, we can see the tilted cross view of

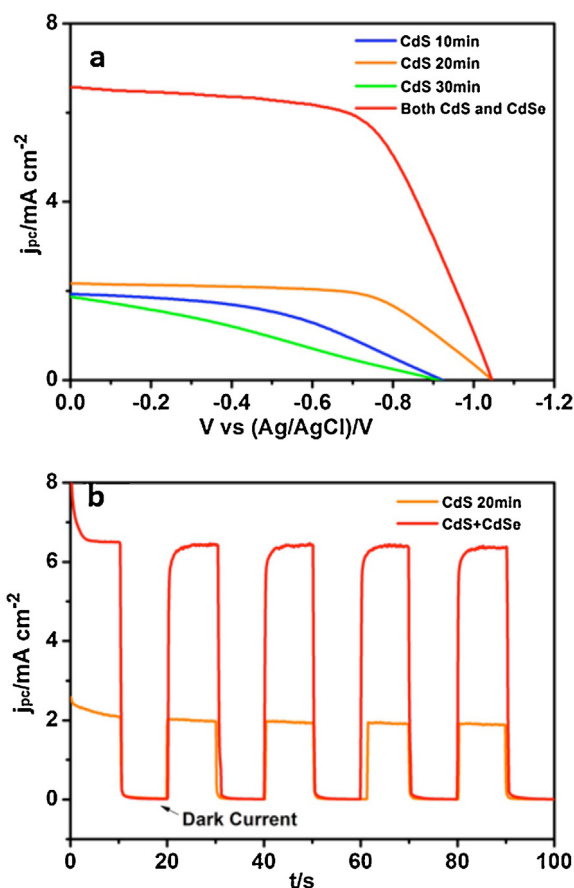


Fig. 4. Photocurrent density-output potential difference (j - V) curves of TiO_2 nanorod array photoanodes covered with CdS shells deposited 10, 20 and 30 min, and CdS/CdSe shells deposited 20 min of each shell successively (a); Photocurrent density response of TiO_2/CdS and $\text{TiO}_2/\text{CdS}/\text{CdSe}$ nanocable arrays (b).

the $\text{TiO}_2/\text{CdS}/\text{CdSe}$ nanocable arrays with the coated of the CdS shells and the CdSe shells for 20 min successively in the Fig. 3c and d. In the Fig. 3d, it clearly shows the top of the $\text{TiO}_2/\text{CdS}/\text{CdSe}$ nanocable arrays became even rougher which were compactly covered with the CdS and CdSe shells.

3.4. TEM and HRTEM observations

Further microscopic characterizations of the TiO_2/CdS and the $\text{TiO}_2/\text{CdS}/\text{CdSe}$ nanocable arrays were displayed by using TEM and high-resolution TEM (HRTEM). The TEM image in Fig. 3g shows a representative single TiO_2/CdS nanocable, and we can see the CdS shell about 15–20 nm thick coated all over the TiO_2 nanorods. The shells are visible as the dark bands on the surface of the nanorods. Fig. 3e shows an HRTEM image in which the interface of the TiO_2 core and the CdS shell can be clearly distinguished for a high crystallinity of the nanocables. The lattice fringes of rutile TiO_2 (001) and CdS (100) with *d* spacings of 0.29 nm and 0.36 nm are denoted in the figure. Fig. 3h shows several representative $\text{TiO}_2/\text{CdS}/\text{CdSe}$ nanocables; the shells coated perfectly on the TiO_2 surface with a thickness of 25–30 nm. Fig. 3f shows the edge of a nanocable, and indicates that the nanocables are highly crystallized. The measured lattice spacings in Fig. 3f are consistent with the *d*-spacings of TiO_2 , CdS, and CdSe. Definitely speaking, the lattice fringes with interplanar spacing $d(001)=0.29\ \text{nm}$ in the upper right of Fig. 3f are consistent with the rutile phase of TiO_2 (JCPDS 88-1175), while $d(100)=0.36\ \text{nm}$ corresponds to the hexagonal phase of CdS (JCPDS 77-2306), and $d(111)=0.35\ \text{nm}$

Table 1
Photovoltage characteristics of TiO₂ nanorod arrays photoanodes covered with CdS shells deposited 10, 20 and 30 min, and CdS/CdSe shells deposited 20 min successively.

| Sample | Photocurrent density/mA cm ⁻² | Output potential difference V vs (Ag/AgCl)/V | Fill factor |
|--------------------------|--|--|-------------|
| CdS 10 min | 1.93 | 0.92 | 0.45 |
| CdS 20 min | 2.17 | 1.04 | 0.62 |
| CdS 30 min | 1.87 | 0.92 | 0.29 |
| CdS 20 min + CdSe 20 min | 6.57 | 1.04 | 0.63 |

corresponds to the face-centered form of CdSe (JCPDS 19-191). Compared with the TiO₂/CdS/CdSe samples which have three different interfaces (TiO₂/CdS, CdS/CdSe, and TiO₂/CdSe) fabricated by SILAR [3], in our prepared nanocables, the CdS shells which were further deposited with CdSe shells had been perfectly coated all over the TiO₂ surface without any blank areas, indicating that the photo-excited electrons completely transfer following the process shown in *Scheme 1*.

3.5. Photovoltaic performance of the electrodes

Fig. 4a shows the photocurrent density-output potential difference (*j*-*V*) curves of the TiO₂/CdS nanocable arrays covered with different thicknesses of the CdS shells and the TiO₂/CdS/CdSe nanocable arrays under AM1.5G simulated sunlight produced by a Zolix SS150 Solar Simulator with an illumination intensity of 100 mW/cm². The photovoltage characteristics of all the nanocables including photocurrent density (*j_{pc}*), output potential difference (*V* vs (Ag/AgCl)/V), and fill factor (FF), are summarized in *Table 1*. It is shown that, with the increase of the deposition time, photocurrent density, output potential difference, and fill factor of the TiO₂/CdS nanocables arrays increase slightly at first and then decrease. It is because the thin CdS shells can broaden the absorbed spectrum region of TiO₂ and promote the transfer of photo-excited electrons through both the TiO₂/CdS interface and the CdS/electrolyte by minimizing electron-hole recombination. However, thicker CdS shells will induce longer transportation path which acts as a potential barrier, causing the recombination of photogenerated electron-hole pairs before they are separated and collected. Therefore, the photocurrent density decreased after the deposition of thicker CdS layers. The optimal photocurrent density of 2.17 mA/cm², output potential difference of 1.04 V and fill factor of 62%, were obtained for the photoanode of the TiO₂/CdS core-shell nanocable array with 20 min CdS deposition. After covered with the CdSe shell over the TiO₂/CdS nanocable arrays, the photocurrent density increased obviously from 2.17 to 6.57 mA/cm², while the output potential difference and fill factor remain the same.

The photocurrent responses under illumination of 100 mW/cm² are shown in the *Fig. 4b*, tested in the polysulfide electrolyte consisting of 0.25 M Na₂S and 0.35 M Na₂SO₃ solution in deionized water, and respectively got by the TiO₂/CdS (orange line) and TiO₂/CdS/CdSe nanocable arrays (red line). Meanwhile, it is clearly observed that the currents are alternated rapidly for the quick transfer of photogenerated electrons from the nanocable arrays to FTO, and there are promising uses of these nanostructures, such as photoelectrochemical, photovoltaic and photocatalysis cells.

Our device configuration is depicted in *Scheme 1*. The conduction band position of CdS is higher than that of TiO₂ but is lower than that of CdSe for the realigned Fermi level. The Fermi levels of the semiconductors normally will be identical after electrostatic equilibrium and thus cause downward or upward shifts of the band edges, when a semiconductor is brought into the contact with another one. In the TiO₂/CdS nanocable arrays, when incident photons are absorbed by the CdS shells, the photo-excited electrons on the conduction band of CdS will quickly inject into the conduction band of the TiO₂, and the energy of the photo-excited electrons decreases. In this mode, photo-excited electron-hole

pairs have been separated and transported respectively to the opposite electrodes. With the stepwise band-edge structure, the TiO₂/CdS/CdSe nanocable arrays show a similar mode as before. Furthermore, compared with CdS shells, CdSe shells have broadened the spectral response region, and the stepwise band-edge structure has a higher performance of the co-sensitized electrode by creating an efficient charge transfer channel.

4. Conclusions

In summary, high-quality TiO₂/CdS and TiO₂/CdS/CdSe nanocable arrays were fabricated by electrochemical deposition method. This method is facile and labor-saving, and it can improve the coverage of CdS shell and CdS/CdSe shell on the surface of TiO₂ nanorod arrays effectively. Perfect TiO₂/CdS/CdSe nanocable arrays with the CdS shell and CdSe shell deposited all over TiO₂ successively without any blank areas were obtained, and this nanostructure formed stepwise band-edge electronic structure as we designed that promoted the quick transfer of the photo-excited electrons. As the result, the TiO₂/CdS/CdSe nanocable arrays reached the photocurrent density of 6.57 mA/cm² and an output potential difference of 1.04 V. This method can be used to fabricate other nanocable arrays.

Acknowledgements

This work was financially supported by the National 863 Program (2011AA050509), the National Natural Science Foundation of China (61106039, 51272084, 61306078, 61225018, 61475062), the National Postdoctoral Foundation (2011049015), the Jilin Province Key Fund (20140204079GX), the State Key Laboratory on Integrated Optoelectronics (IOSKL2012ZZ12), the Taishan Scholarship, the Shandong Natural Science Foundation (ZR2012FZ007), and the NSF (1338346).

References

- [1] A. Kongkanand, K. Tvrđy, K. Takechi, M. Kuno, P.V. Kamat, Quantum dot solar cells. Tuning photoresponse through size and shape control of CdSe-TiO₂ architecture, *J. Am. Chem. Soc.* 130 (2008) 4007.
- [2] I. Robel, V. Subramanian, M. Kuno, P.V. Kamat, Quantum dot solar cells. Harvesting light energy with CdSe nanocrystals molecularly linked to mesoscopic TiO₂ films, *J. Am. Chem. Soc.* 128 (2006) 2385.
- [3] S.L. Cheng, W.Y. Fu, B.Y. Hai, L.N. Zhang, J.W. Ma, H. Zhao, M.L. Sun, L.H. Yang, Photoelectrochemical performance of multiple semiconductors (CdS/CdSe/ZnS) cosensitized TiO₂ photoelectrodes, *J. Phys. Chem. C* 116 (2012) 2615.
- [4] H. Chen, W.Y. Fu, H.B. Yang, P. Sun, Y.Y. Zhang, L.R. Wang, W.Y. Zhao, X.M. Zhou, H. Zhao, Q.A. Jing, X.F. Qi, Y.X. Li, Photosensitization of TiO₂ nanorods with CdS quantum dots for photovoltaic devices, *Electrochim. Acta* 56 (2010) 919.
- [5] B. Wen, C. Liu, Y. Liu, Depositional characteristics of metal coating on single-crystal TiO₂ nanowires, *The Journal of Physical Chemistry B* 109 (2005) 12372.
- [6] K. Shankar, J.I. Basham, N.K. Allam, O.K. Varghese, G.K. Mor, X. Feng, M. Paulose, J.A. Seabold, K.-S. Choi, C.A. Grimes, Recent advances in the use of TiO₂ nanotube and nanowire arrays for oxidative photoelectrochemistry, *J. Phys. Chem. C* 113 (2009) 6327.
- [7] H. Wang, Y. Bai, H. Zhang, Z. Zhang, J. Li, L. Guo, CdS quantum dots-sensitized TiO₂ nanorod array on transparent conductive glass photoelectrodes, *J. Phys. Chem. C* 114 (2010) 16451.
- [8] Q. Shen, J. Kobayashi, L.J. Diguna, T. Toyoda, Effect of ZnS coating on the photovoltaic properties of CdSe quantum dot-sensitized solar cells, *J. Appl. Phys.* 103 (2008) .
- [9] C.F. Chi, H.W. Cho, H. Teng, C.Y. Chuang, Y.M. Chang, Y.J. Hsu, Y.L. Lee, Energy level alignment, electron injection, and charge recombination characteristics

- in CdS/CdSe cosensitized TiO₂ photoelectrode, *Applied Physics Letters* 98 (2011) .
- [10] J.H. Bang, P.V. Kamat, Quantum dot sensitized solar cells. A tale of two semiconductor nanocrystals: CdSe and CdTe, *ACS Nano* 3 (2009) 1467.
- [11] R. Plass, S. Pelet, J. Krueger, M. Grätzel, U. Bach, Quantum dot sensitization of organic-inorganic hybrid solar cells, *The Journal of Physical Chemistry B* 106 (2002) 7578.
- [12] Y. Zhang, Q. Dai, X. Li, J. Liang, V.L. Colvin, Y. Wang, W.W. Yu, PbSe/CdSe and PbSe/CdSe/ZnSe hierarchical nanocrystals and their photoluminescence, *Langmuir* 27 (2011) 9583.
- [13] R.D. Schaller, V.I. Klimov, High efficiency carrier multiplication in PbSe nanocrystals: Implications for solar energy conversion, *Phys. Rev. Lett.* 92 (2004) .
- [14] G. Wang, X. Yang, F. Qian, J.Z. Zhang, Y. Li, Double-sided CdS and CdSe quantum dot co-sensitized ZnO nanowire arrays for photoelectrochemical hydrogen generation, *Nano Lett.* 10 (2010) 1088.
- [15] Z. Zhu, J. Qiu, K. Yan, S. Yang, Building high-efficiency CdS/CdSe-sensitized solar cells with a hierarchically branched double-layer architecture, *ACS Applied Materials & Interfaces* 5 (2013) 4000.
- [16] C.H. Chang, Y.L. Lee, Chemical bath deposition of CdS quantum dots onto mesoscopic TiO₂ films for application in quantum-dot-sensitized solar cells, *Applied Physics Letters* 91 (2007) .
- [17] S. Gimenez, T. Lana-Villarreal, R. Gomez, S. Agouram, V. Munoz-Sanjose, I. Mora-Sero, Determination of limiting factors of photovoltaic efficiency in quantum dot sensitized solar cells: Correlation between cell performance and structural properties, *J. Appl. Phys.* 108 (2010) .
- [18] H. Lee, M. Wang, P. Chen, D.R. Gamelin, S.M. Zakeeruddin, M. Graetzel, M.K. Nazeeruddin, Efficient CdSe quantum dot-sensitized solar cells prepared by an improved successive ionic layer adsorption and reaction process, *Nano Lett.* 9 (2009) 4221.
- [19] L.J. Diguna, Q. Shen, J. Kobayashi, T. Toyoda, High efficiency of CdSe quantum-dot-sensitized TiO₂ inverse opal solar cells, *Applied Physics Letters* 91 (2007) .
- [20] B. Farrow, P.V. Kamat, CdSe quantum dot sensitized solar cells. Shuttling electrons through stacked carbon nanocups, *J. Am. Chem. Soc.* 131 (2009) 11124.
- [21] X.Y. Yu, J.Y. Liao, K.Q. Qiu, D.B. Kuang, C.Y. Su, Dynamic study of highly efficient CdS/CdSe quantum dot-sensitized solar cells fabricated by electrodeposition, *ACS Nano* 5 (2011) 9494.
- [22] Z. Lu, J. Xu, X. Xie, H. Wang, C. Wang, S.-Y. Kwok, T. Wong, H.L.I. Kwong Bello, C.-S. Lee, S.-T. Lee, W. Zhang, CdS/CdSe double-sensitized ZnO nanocable arrays synthesized by chemical solution method and their photovoltaic applications, *The Journal of Physical Chemistry C* 116 (2011) 2656.
- [23] J.Q. Zhang, J.Y. Yang, M. Liu, G. Li, W.X. Li, S. Gao, Y.B. Luo, Fabrication of CdTe quantum dots sensitized TiO₂ nanorod-array-film photoanodes via the route of electrochemical atomic layer deposition, *J. Electrochem. Soc.* 161 (2014) D55.
- [24] X. Wang, H. Zhu, Y. Xu, H. Wang, Y. Tao, S. Hark, X. Xiao, Q. Li, Aligned ZnO/CdTe core-shell nanocable arrays on indium tin oxide: Synthesis and photoelectrochemical properties, *ACS Nano* 4 (2010) 3302.
- [25] B. Liu, E.S. Aydil, Growth of oriented single-crystalline rutile TiO₂ nanorods on transparent conducting substrates for dye-sensitized solar cells, *J. Am. Chem. Soc.* 131 (2009) 3985.